

The Perennial Ice Cover of the Beaufort Sea from Active and Passive Microwave Observations

R. Kwok

*Jet Propulsion Laboratory, California Institute of Technology
4800 Oak Grove Drive, Pasadena, CA 91109*

J. C. Comiso

*Laboratory for Hydrospheric Processes, Goddard Space Flight Center
Greenbelt, MD 20771*

ABSTRACT. We examine the perennial ice concentration in the Beaufort Sea using active and passive microwave observations. The definition of multiyear ice provides a condition which states that area of multiyear ice during the winter should be nearly equivalent to the ice area during the previous summer's minima. We compare the ice type and concentration estimates from SSM/I and ERS-1 SAR data over a seasonal cycle from January 1992 to January 1993. We found that the multiyear ice concentration estimates from the SAR data to be very stable and are nearly equivalent to the ice concentration estimated at the end of the previous summer. We contrast this with the variability of the MY ice concentration and ice fraction estimates obtained using SSM/I data. The passive microwave algorithms provides ice concentration and multiyear ice estimates which are consistently lower than those from the SAR data. We discuss reasons for these discrepancies and the possible biases introduced by the active and passive algorithms.

If records of the Team algorithm results are examined, one finds that the estimates of multiyear (MY) ice concentration in the winter are much lower (by up to 30%) than that of the summer ice concentration. From an ice balance perspective, such large discrepancies need to be resolved. If ice which survives the summer is classified as MY ice, then the MY ice concentration during the winter should be nearly equivalent to the ice concentration during the previous summer's minima, differing by an amount due to melt, ridging, new/young ice formation and export of ice from the Arctic. This mismatch was noted by a number of investigators from the point of view of this variability of the multichannel microwave signatures of sea ice on regional studies [77,0f/tas,1993], from comparison with surface measurements [Grenfell and Lohanick, 1985; Grenfell, 1992], and from an ice balance perspective [Comiso, 1990; Rothrock and Thomas, 1990; 771 mas and Rothrock, 1993].

1 Introduction

The radar imagery from the ERS-1 Synthetic Aperture Radar (SAR) provides an alternate view of the sea ice cover in addition to the relatively long record provided by the SSM/I multichannel radiometer. The operational NASA sea ice algorithm or Team algorithm [Cavalieri *et al.*, 1984] routinely estimates ice type and ice concentrations from passive microwave observations. However, the procedures used to estimate these same parameters from active microwave observations (Kwok *et al.* [1992], Comiso and Kwok, [1993]) are still relatively new. Large scale (temporal and spatial) comparative studies between the estimates from the active and passive datasets are limited by the coverage and the data volume of high resolution ERS-1 SAR data. The objectives of this study are: to compare the retrieval results obtained using the active and passive procedures; to understand the physical meaning of these differences; and, their implication about the state of the ice cover.

Data Description

The comparative analysis of the active and passive ice type and concentration estimates was done in the region shown in Fig. 1. This covers an area of approximately 1500 km by 900 km. The region is selected based on the dataset available to us, at the time of this study, through the Alaska SAR Facility. All data used here were acquired between January 1992 and January 1993.

Gridded SSM/I brightness temperatures from a 11 SSM/I channels were used in the ice type and open water retrievals. Daily averages were mapped to a 304 by 448 matrix with a grid size of 25 km by 25 km. The 19 and 37 GHz channels were used in the retrieval of total and MY ice concentrations and the 22 GHz channel was to provide an ocean mask.

A total of 571 ERS-1 SAR images, approximately 44

images per month, were used in this study. The ERS-1 SAR is a C-band (5.3 GHz) radar operated with vertical transmit and receive polarizations at a look angle close to 90° . The antenna's elevation beam illuminates an across track swath of approximately 100 km in width. The image data used in this study were received and processed at the Alaska SAR Facility (ASF) in Fairbanks, Alaska. Ancillary data are provided with each image product for calibration and conversion of the 8-bit digital data into normalized backscatter cross sections.

Data Analysis

We use the NASA Team algorithm [Cavalieri *et al.*, 1984; Gloersen and Cavalieri, 1986] to compute the concentration of open water, first-year (FY) ice and MY ice at each 25 km cell. The Team algorithm is based on a mixing formulation to resolve the MY ice, FY ice and open water within each grid element. The ice and water signatures are assumed to have temporally and spatially stable gradient and polarization ratios. The precision of the open water estimates, in the Beaufort and Chukchi Seas, ranges between -2.143.1% and 0.6-7.4% [Cavalieri, 1992]. The variance in the MY ice estimates, when compared with estimates from other sensors, are higher and trends are not evident. The reader is referred to Cavalieri [1992] for a summary of the differences between the Team algorithm ice concentrations and those derived by other sensors.

We use a backscatter-based classification algorithm (described in Kwok *et al.* [1992]) to identify ice types in the SAR data. Each pixel is classified into one of the three categories: MY, FY and smooth ice/open water. No attempt is made to resolve the mixture of ice types within a pixel. The persistent backscatter contrast between MY ice and FY ice [Kwok and Cunningham, 1994] was used to as a discriminant between the two ice types. The winter algorithm sometimes fails to correctly classify open water and new ice due to overlap in their backscatter distributions. Fetterer *et al.* [1994] assessed the performance of this algorithm and reported that the precision of MY ice concentration estimates are better than 6%. In their comparative study with Landsat data, Steffen and Heinrichs [1994] pointed out that FY ice and old ice could be clearly separated based on their scattering coefficients; their study showed an error of 58% for compact ice conditions. Our evaluation of the MY ice retrieval procedure, using ten pairs of SAR image data of the geographic location from the 3 day ERS-1 repeat cycle, show differences of less than 1%. The results suggest that the signatures are stable at least over the short term and that the higher uncertainty observed by Fetterer *et al.* [1994] could be due to a combination of spatial and temporal variability of the ice signature over the longer term. The higher than

normal backscatter of frost-flower covered sea ice could also be problematic due to their time-dependent signature [Kwok and Cunningham, 1993], but we expect that the area fraction of this ice category to be less than a few percent in the winter Arctic away from the coast. A limitation with this backscatter-based classification is the potential confusion between deformed FY ice and MY ice especially in the region of transition between the seasonal and perennial ice zones [Rignot and Drinkwater, 1994]. Both ice types have similar backscatter and based on their analysis of aircraft SAR data, the MY ice concentration could be overestimated by as much as 15%.

Only ice concentration is derived from SAR data in the summer. After the onset of melt in the spring, the contrast between FY and MY ice at C-band is lost and there is at present no effective means for ice type classification in the summer time. The summer sea ice cover at C-band has an average range of backscatter that is between -17 dB and -12 dB. At C-VV, open water backscatter is dependent on wind speed and is typically higher than that of the ice cover if the wind speed is above 4-5 m/s. The azimuthal look direction introduces only 1-2 dB of modulation of the backscatter at ERS-1 look angles. We estimate open water in leads by using an algorithm [Comiso and Kwok, 1993] which takes advantage of the higher backscatter of wind-roughened open water relative to the ice cover. Using wind speed as an initial guess, the thresholds are adjusted visually to discriminate between water and ice. The precision of our ice concentration estimates are approximately 2-3% during windy conditions (above 4-5 m/s). During calm conditions ice concentrations are also derived, but the uncertainties are higher because of the decrease in contrast. The precision of under these conditions, based on repeated visual classification of these images, is approximately 10%. Since melt ponds are blended in with the backscatter of ice and snow on ice floes, the melt ponds are classified as sea ice in our algorithm. However, sub-resolution leads are not accounted for and contribute to overestimates of the ice concentration. More extensive observations, preferably airborne surveys, are necessary to better quantify this error.

Results and Discussion

Coincident ice type and concentration data derived from both SAR and SSM/I data are plotted in Fig. 2. The region of study is divided into five latitude bands with intervals of 2.5° starting at 70°N . The ice concentration results from both procedures were generally consistent except during the summer, while the MY ice concentrations differ substantially.

In the winter (from Jan-May), the total ice concentra-

tions agree to within the uncertainty of the estimates at all latitude bands. The Beaufort Sea is almost 100% ice-covered. When data points lie outside the region of validity in gradient and polarization space, the Team algorithm occasionally provides anomalous estimates of ice concentrations that are greater than 100% during the winter.

The MY ice concentrations from the two analyses, however, are quite different. The SAR-derived MY ice concentrations are quite stable at the higher latitudes and there is no significant increase or decrease in the amount of MY ice except near the transition between the perennial pack and the seasonal ice zone. These MY concentrations are consistent with ice kinematics during this period and our expectation that this parameter stays fairly constant, especially in this part of the Beaufort Sea and the central Arctic. Within the two lowest latitude trends, we attribute the variability to the advection of MY and FY ice into and out of the region of study and possibly to the ridging of FY ice.

The Team algorithm results as shown in Fig. 2 indicate a trend of decreasing MY ice concentration at the higher latitude bands. Between 75°N and 77.5°N, there is a greater than 30% decrease in the MY ice concentration between January and May. We check qualitatively to see whether this decrease is consistent with ice kinematics. During this period (between September 1, 1991 and April 1, 1992) the ice cover is actually slightly convergent (~10%) which should yield an increase rather than a decrease in the MY ice concentration. With a mean velocity of 2 cm/s, the total displacement of the ice is less than 240 km, which is small compared to our region which encompasses an area of 1500 km by 900 km. It is difficult to explain this trend from the perspective of ice cover divergence or a net advection of MY ice out of our study region.

Could the decreasing trend be explained if ice advection and divergence were not the causes? We examine (Fig. 3) the daily gradient and polarization ratios of three 100 km x 100 km regions centered at the following geographic locations: A(80°N, 130°W), B(77.5°N, 135°W) and C(75°N, 140°W). At high ice concentrations in the winter, the gradient ratio is the principal parameter which allows the separation of MY ice from FY ice. In addition to the small amplitude variations, there is a slowly increasing trend in this parameter in all three regions and is especially obvious after day 100. The gradient ratio varies between 0 for 100% FY ice and -0.09 for 100% MY ice. Any increase in this ratio would tend to decrease the estimated MY ice concentration. At 100% ice concentration, an increase of 0.01 in the gradient ratio would decrease the estimated MY ice concentration by approximately 11%. The increasing

gradient ratio in the spring (before melt onset) would therefore cause a decrease in the amount of MY ice in the region. We do not speculate here on the reasons for the increasing gradient ratio except that the probable causes are surface or atmospheric effects.

Only a comparative analysis of total ice concentrations is possible since neither the active or passive algorithms can estimate ice type concentration in the summer. *Comiso and Kwok* [1993] provide a more comprehensive analysis of the differences between active and passive observations for this summer period. After the onset of melt in spring, there is a gradual increase in the areal fraction of open water. The SAR-derived ice concentrations are typically higher than those of the Team algorithm estimates and the differences are more pronounced at lower latitudes. A possible cause of this [discussed in *Comiso and Kwok*, 1993] is the contribution of melt ponds to the open water estimates. Water in melt ponds has the same passive microwave signature as that of water in open leads causing an underestimation of ice concentration. The larger difference in the lower latitude bands may be indicative of the latitude dependence of melt pond fraction. We note again that the SAR estimates are biased toward over-estimation of ice concentration because sub-resolution open leads are most likely classified as ice in the summer time. We do not know, in the current observational literature, the relative area contribution of sub-resolution leads and melt ponds in the summer. If the contribution is small as we discussed earlier, for melt pond concentrations of 20-30% the melt ponds would seem to be the dominant factor which affect the microwave signatures. In other words, the underestimation of the Team algorithm is more significant than the bias introduced by small leads. These biases can only be resolved with high resolution aerial survey.

At the end of the summer, the surviving ice from the previous spring becomes MY ice. The SAR results show that the MY ice concentration in early October is roughly equivalent to the SAR-derived ice concentration at summer's end. Based on the SAR analysis, the ice cover seems to be fairly compact with high concentrations of MY ice at all latitude bands. In the following months, the concentration decreases (especially at the lower latitude-s) and returns to a level comparable to that of the previous winter. We attribute this decrease to a convergence in the ice cover in the summer followed by a divergence of the ice cover in November and December. Indeed, the velocity fields (between April 1 - September 1, 1992) also indicate a convergence of the ice cover in this region of approximately 10-20% in the summer in the lower latitudes and divergence of a smaller magnitude in the fall. The highly compact ice cover (high ice concentration) can be seen in the SAR image data. At this time, the ice cover seems to be

composed of primarily MY ice with low FY ice concentration. In October, the ice cover has low FY ice concentrations whereas in December the characteristic FY ice signature (lower backscatter) is more evident due to the thickening of the ice in the open leads created in the previous months. The ice cover attains a backscatter character, in terms of MY ice and FY ice concentrations, that is similar to that of the previous winter.

The Team algorithm provide substantially different (about 50%) ice concentrations at the end of the summer and the MY ice concentration during the subsequent winter. Such a mismatch could only occur if ice growth can occur simultaneously with the melt of a large percentage of MY ice. From the time sequence (Fig. 2), it is difficult to explain how melt and freeze-up of such magnitude could occur in the region. Our expectation is that the amount of MY ice should remain fairly constant especially in the higher latitudes in the central Arctic.

There is also a large difference between MY ice concentration estimates from the SAR and the Team algorithms. The differences are likely due to the spatial variations in the emissivity of sea ice in the Arctic region [Carsey, 1982; Comiso, 1983]. One factor which causes such spatial changes in the emissivity is melting since frozen meltponds are known to have emissivities of first year ice [Grangfeld, 1992]. This can be a substantial effect since 20-30% of the summer ice have been observed to be ponded [Tucker, private communication, 1994]. It is not clear, however, how many of these meltponds survive into the winter. Another factor could be unusually thick snow cover in some areas that can cause flooding (and subsequent refreezing) at the snow ice interface. Such effects cause the snow/ice interface to be saline and the emissivity of the ice floe to be similar to that of FY ice.

Do the SAR algorithms overestimate MY ice concentration? It has been reported [Rignot and Drinkwater, 1994] that deformed FY ice has backscatter characteristics similar to that of MY ice in single polarization C-band datasets like ERS-1. This would cause the SAR winter algorithm to overestimate the MY ice concentration. If this is the case, due to deformation of the ice cover, the amount of deformed ice should increase as the winter wears on resulting in a gradual increase in the estimated MY ice concentration. Indeed we do not observe such trend, at least not within the level of uncertainty of the estimates. We discuss the effect of the ridging process with an example. If there is a 15% convergence of the ice cover and this FY ice area is converted into deformed ice, what is the expected bias in the MY ice concentration if the signature of de-

formed ice is identical to that of FY ice? When FY ice ridges, and here we assume that we only ridge the very thin ice from closing of leads, the area is not conserved. The mechanical thickness redistribution takes the volume of ice participating in a ridging event and creates an approximately equivalent volume of ice occupying a smaller area. As a crude estimate, if we use the assumption that all ridged ice is five times its original thickness before ridging (parameter used by Thorndike *et al.*, 1975) then the contribution of the FY ice area after convergence is much smaller. The 5% undeformed ice area now occupies an area of 3%.

This leads to a very interesting question. If large volumes of FY ice are piled onto MY ice, do we label this area as MY ice or FY ice? The SAR algorithms described here would label the area as MY. The passive algorithms might label that area differently depending on the emissivity of that ice. If the FY ice desalates quickly by gravity drainage, would that not look like MY ice? It does not seem to be important from the heat flux point of view because thick ice has a relatively small contribution to the total flux, but certainly important from the mass balance point of view. It is possible that deformed FY ice is piled onto the MY ice and therefore do not increase the concentration of MY ice even though the polarimetric radar senses a surface type [Rignot and Drinkwater, 1994] which seems to be different than that of MY ice. We do not know the areal contribution of this deformed FY/MY ice type. If the areal fraction of this surface type is significant, it would affect the passive microwave retrieval algorithms as well.

Summary/Discussion

Over the annual cycle, the total ice concentration remained fairly high in our region of study. From the Team algorithm estimates, we observe a significant decrease in the amount of MY ice (almost 40%) between January and spring melt and a slower increase in the amount of MY ice between September and December. The MY ice concentration at freeze up is much lower than the ice concentration at the end of summer, an inconsistency in the analysis which suggests an underestimation of MY ice in the winter time. Meltponds and other surface effects seem to contribute significantly to the underestimation of ice concentration in the summer.

The SAR analyses suggest an ice cover in the Beaufort which is rather stable, throughout a season, in terms of MY ice concentration. The amount of MY ice remained approximately constant, within the level of uncertainty of the analysis. The average MY ice concentration in this part of the Arctic Ocean is approximately 80%. At the end of the summer, the MY ice concentration

is approximately equivalent to the ice concentration at the end of the summer. These analyses seem to give a consistent view of the annual cycle. The C-band radar, to first-order, is not affected by snow cover when the temperature is below freezing and much less sensitive to weather effects than the higher frequency radiometer channels. The equivalence between summer ice minima and winter MY ice concentration, and the small fluctuations in the SAR estimates in the winter lead us to believe that these estimates are at least consistent. At this point, the analysis of the SAR data offers another estimate of the MY ice, which seems to be consistent with the summer ice concentration. If the SAR is correct, then the Team algorithm underestimates the MY ice by even a larger amount than previous studies have shown and imply a higher MY ice concentration in the Beaufort Sea.

Because meltponds have signatures of open water and the Team algorithm does not discriminate between the two surface types, it underestimates the ice concentrations in the summer. If the meltpond concentration is 30%, then the ice concentration would be underestimated by a similar amount. This is consistent with the differences between the SAR analysis and the Team algorithm analysis: the SAR estimates of total ice concentration is always higher than that of the Team algorithm estimates in the summer. If Team algorithm underestimates the total ice concentration due to meltponds, especially in the ice margin in the summer, then computed total ice area would also be underestimated.

The estimates from the SAR and Team algorithms provided two fairly different views of the Beaufort Sea ice cover. The limitations of both algorithms were discussed. The differences explain some of the possible biases of these algorithms due to variability in signature as functions of wavelength and environmental conditions. Future investigations using these datasets should be cautious of the possible biases introduced by these analysis algorithms.

Acknowledgments

R. Kwok performed this work at the Jet Propulsion Laboratory, California Institute of Technology under contract with the National Aeronautics and Space Administration. J. C. Comiso performed this work at the Laboratory for Hydrospheric Processes at NASA Goddard Space Flight Center. This project was supported by the NASA Cryospheric Processes Program under R. H. Thomas.

References

- Carsey, P. D., Arctic sea ice distribution at end of summer from satellite microwave data, *J. Geophys. Res.*, 87(C8), 5809-5835, 1982.
- Cavalieri, D. J., P. Gloersen and W. J. Campbell, Determination of sea ice parameters from Nimbus 7 SMMR, *J. Geophys. Res.*, 89(14), 5355-5369, 1984.
- Cavalieri, D. J., The validation of geophysical products using multisensor data, in *Microwave Remote Sensing of Sea Ice*, Ed. P. D. Carsey, (Geophysical Monograph 68, AGU, 1992).
- Comiso, J. C., Sea ice microwave emissivities from satellite passive microwave and infrared observations, *J. Geophys. Res.*, 88(C12), 7686-7704, 1983.
- Comiso, J. C., Arctic multiyear ice classification and summer ice cover using passive microwave satellite data, *J. Geophys. Res.*, 95(C8), 13411-13422, 1990.
- Comiso, J. C. and R. Kwok, Summer Arctic Ice Concentrations and Characteristics from SAR and SSM/I First ERS-1 Symposium, ESA SP-350, Cannes, 367-372, 1993.
- Fetterer, F. D. Gineris and R. Kwok, Sea ice type maps from Alaska synthetic aperture radar facility imagery: A first assessment, *J. Geophys. Res.*, 99(C11), 22443-22458, 1994.
- Gloersen, P. and D. J. Cavalieri, Reduction of weather effects in the calculation of sea ice concentration from microwave radiances, *J. Geophys. Res.*, 91(C3), 3913-3919, 1986.
- Grenfell, T. C., Surface-based passive microwave observations of sea ice in the Bering and Greenland Seas, *IEEE Trans. Geosci. Remote Sens.*, GE-24(6), 826-831, 1986.
- Grenfell, T. C., Surface-based passive microwave studies of multiyear ice, *J. Geophys. Res.*, 97(C3), 3485-3501, 1992.
- Grenfell, T. C. and A. W. Lohanick, Temporal variations of the microwave signatures of sea ice during the late spring and early summer near Mould Bay NW1, *J. Geophys. Res.*, 90(C3), 5063-5074, 1985.
- Kwok, R. and G. F. Cunningham, Backscatter Characteristics of the Winter Sea Ice Cover in the Beaufort Sea, *J. Geophys. Res.*, 99(C4), 7787-7803, 1994.
- Kwok, R., E. Rignot, B. Holt and R. G. Onstott, Identification of Sea Ice Types in Spaceborne SAR Data, *J. Geophys. Res.*, 97(C2), 2391-2402, 1992.
- Kwok, R. and G. F. Cunningham, Use of Time Series SAR Data To Resolve Ice Type Ambiguities in Newly-opened Leads, *Proceedings of IGA RSS'94*, Pasadena, CA, 1024-1026, 1994.

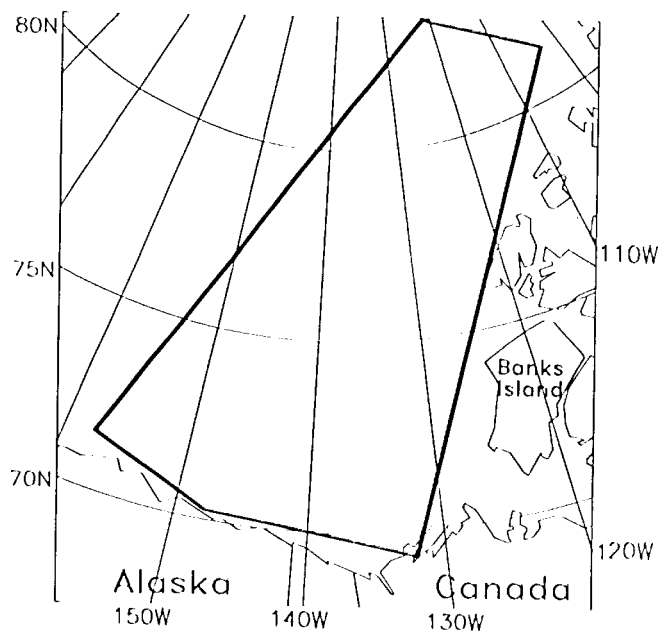
- Rignot, E. and M. Drinkwater, Winter sea ice mapping from multi-parameter synthetic aperture radar, *J. Glaciol.*, 40(134), 3-45, 1994.
- Rothrock, D. A. and D. R. Thomas, The Arctic Ocean multiyear ice balance, 1979-82, *Ann. Glaciol.*, 14, 252-255, 1990.
- Steffen, H. and J. Heinrichs, Feasibility of sea ice typing with synthetic aperture radar (SAR): Merging of Landsat thematic mapper and ERS-1 satellite imagery, *J. Geophys. Res.*, 99(C11), 22413-22424, 1994.
- Thomas, D. R. and D. A. Rothrock, The Arctic Ocean ice balance: A Kalman filter smoother estimate, *J. Geophys. Res.*, 98(C6), 10054-10067, 1993.
- Thomas, D. R., Arctic sea ice signatures for passive microwave algorithms, *J. Geophys. Res.*, 98(C6), 10037-10052, 1993.
- Thorndike, A. S., D. A. Rothrock, G. A. Maykut and R. Colony, The thickness distribution of sea ice, *J. Geophys. Res.*, 80(33), 4501-4513, 1975.

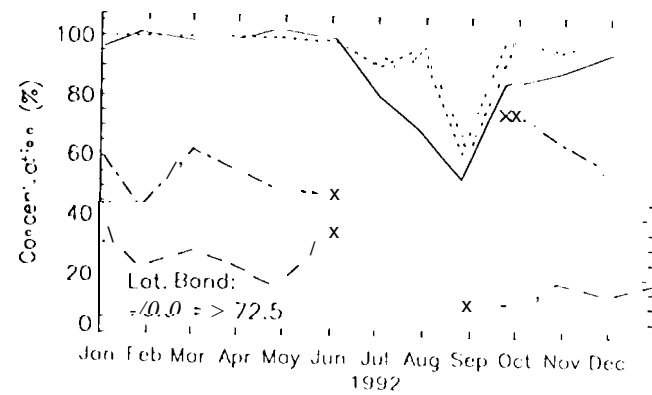
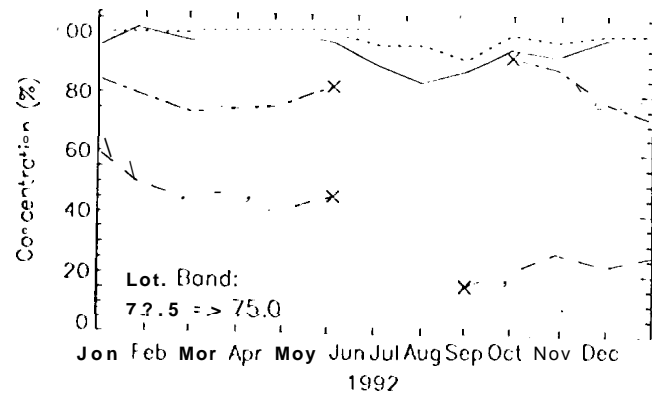
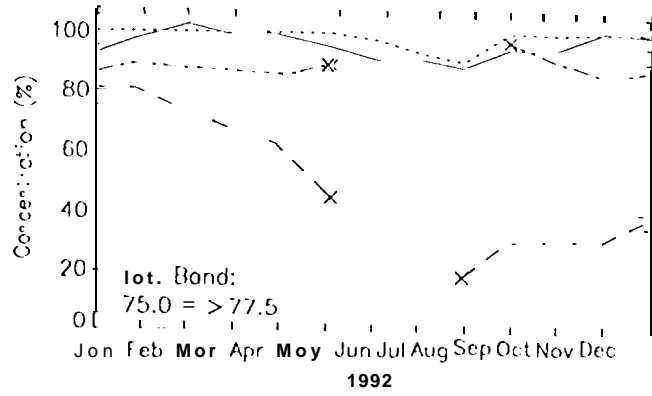
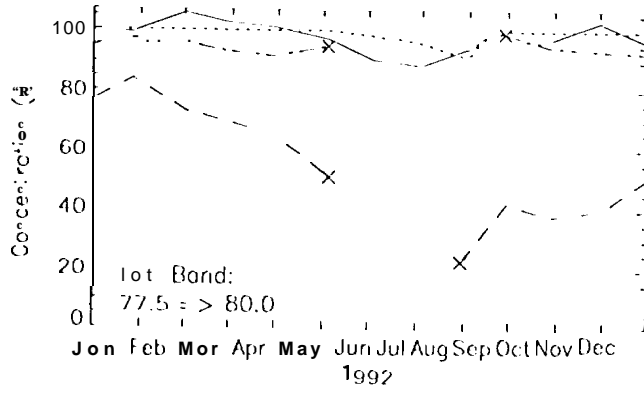
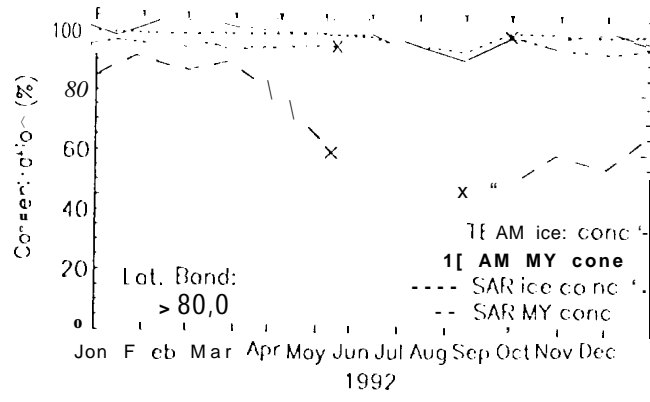
Figure Captions

Figure 1. The comparative analysis uses ERS-1 SAR and SSM/I data from the region defined by these boundaries.

Figure 2. Comparisons of the total ice and multiyear ice concentrations at five latitude bands. (a) 70.0°-72.5°. (b) 72.5°-75.0°. (c) 75.0°-77.5°. (d) 77.5°-80.0°. (e) 80.0°.

Figure 3. Plots of the gradient and polarization centered at three different 100 km by 100 km regions. (a) A (80°N, 130°W). (b) B (77.5°N, 135°W). (c) (75°N, 140°W).





Polarization Ratio (PR) and Gradient Ratio (GR)

